

Nitrogen-doped Carbon-based Very Thin Film on Quartz or Sapphire Substrate as Back-side Illuminated Transmission Photocathode

^{1,2,*} Jozef HURAN, ¹ Nikolay I. BALALYKIN, ¹ Mikhail A. NOZDRIN,
³ Vlasta SASINKOVÁ, ⁴ Angela KLEINOVÁ, ¹ Alexander P. KOBZEV
and ² Eva KOVÁČOVÁ

¹ Joint Institute for Nuclear Research, Joliot-Curie 6, Dubna, 141980, Russian Federation

² Institute of Electrical Engineering, Slovak Academy of Sciences,
Dúbravská cesta 9, Bratislava, 84104, Slovakia

³ Institute of Chemistry, Slovak Academy of Sciences, Dúbravská cesta 9, 84538 Bratislava, Slovakia

⁴ Polymer Institute, Slovak Academy of Sciences, Dúbravská cesta 9, 84541 Bratislava, Slovakia

¹ Tel.: + 74962163843, fax: + 74962165767

E-mail: jozef.huran@savba.sk

Received: 15 April 2019 / Accepted: 28 May 2019 / Published: 31 July 2019

Abstract: Nitrogen-doped carbon-based very thin films were deposited on quartz or sapphire substrate by RF reactive magnetron sputtering using carbon target and gas mixture of Ar and reactive gases N₂ or N₂+H₂. The concentration of elements in the films was determined by RBS and ERD analytical method simultaneously. Carbon-based films surface morphology was examined by scanning electron microscopy. Raman spectroscopy was used for chemical structural properties investigation of carbon films. The photo-electron emission properties were determined by the measurement of cathode bunch charge of prepared back-side pulsed laser illuminated transmission photocathode. Adding hydrogen to gas mixture and changing their flow when carbon films are growth, leads to different results of photo-electron emission properties. Influence of chemical structural properties of N-doped carbon-based very thin films on quartz or sapphire substrates on the photo-induced electron emission of back-side illuminated transmission photocathode are discussed.

Keywords: Carbon very thin film, Magnetron sputtering, Structural properties, Transmission photocathode.

1. Introduction

High quality electron field emitting materials with stable emission are needed for a wide range of applications. Various carbon based materials such as diamond, graphene, carbon nanotubes has received attention as novel electron field emission cold cathodes. To obtain high-power and high-brightness radiation in free-electron lasers, for future electron-

positron colliders, as well as for other applications, the sources of intense electron beams with bunches having a small emittance and a large charge is required [1]. Photocathodes working in reflection mode were made of rich-diamond and rich-graphite nanodiamond layers, deposited on different conductive substrates by means of the pulsed spray technology [2]. The electron field emission behaviors of amorphous carbon, graphene sheets embedded carbon and graphite-like

carbon structures were investigated and the mechanism of enhanced field emission was attributed to the nanosized graphene sheets which acted as electron emitters and transport channels [3]. The results of the quantum efficiency measurements, in the range 150-210 nm, of photocathodes based on poly-, nano- and single crystalline diamond are reported [4]. Electron field emission properties of nanocarbon film produced by PECVD technique were investigated. The film contained nanostructured diamond and graphitic components in different ratios depending on the deposition process parameters [5]. For nitrogen-doped diamond films on metallic substrates, photo-induced electron generation at visible wavelengths involves both the ultra-nanocrystalline diamond and the interface between the diamond film and metal substrate [6]. Authors report field electron emission investigations in Q-carbon composite structures formed by pulsed laser annealing of amorphous carbon layers. Under the optimum fabrication conditions, a dense microstructured morphology of Q-carbon was obtained, which is important for local electric field enhancement in field-emission device applications [7]. To achieve enhanced electron field emission, diamond-graphite nanohybrid films are deposited on Si substrates by means of a microwave plasma chemical vapor deposition (MPCVD) reactor. An increase of deposition temperature from 730 °C to 830 °C leads to remarkable changes of morphology and microstructure of diamond-graphite nanohybrid films [8]. Diamond-like carbon films were deposited on the stainless steel mesh by PECVD technique from gas mixtures $\text{CH}_4+\text{D}_2+\text{Ar}$, $\text{CH}_4+\text{H}_2+\text{Ar}$ and reactive magnetron sputtering using a carbon target and gas mixtures $\text{Ar}+\text{D}_2$, $\text{Ar}+\text{H}_2$, for the transmission photocathode preparation [9]. Nitrogen-doped carbon materials are reviewed by focusing on their preparation and applications. Their preparation is described in the order of graphene, carbon nanotube and fibers, porous carbons and carbon blacks [10]. Raman spectroscopy is a measurement technique that is widely used to study all carbon-based materials and carbon nanostructures and as such is one of the characterization methods that can be used for the analysis of nanocrystalline diamonds. Authors focus on detonation nanodiamonds, the contributions and weaknesses of the method for the understanding of their nanostructure and their surface features are reviewed. The choice of the excitation wavelength, from deep UV to more conventional visible wavelengths, and the choice of the experimental conditions are examined [11]. More generally, Raman spectroscopy is an experimental technique that is now commonly used to characterize all carbon materials and carbon nanostructures from three to zero dimensions (3D, 0D), such as 3D graphite or diamond, 2D graphene, 1D carbon nanotubes, and 0D fullerenes [12].

In this paper, carbon-based very thin films doped with nitrogen were deposited by RF magnetron sputtering on quartz or sapphire substrates. The surface morphology and microstructure of carbon

films are characterized carefully. The prepared back-side illuminated transmission photocathodes was used for investigation of photo-induced electron emission properties of carbon-based films.

2. Experiment

The carbon-based very thin films were grown on double side polished quartz or c-sapphire substrate by RF (radio frequency) reactive magnetron sputtering using gas mixtures Ar, N_2 and H_2 . Stainless steel vacuum chamber was evacuated by turbomolecular pump to a base pressure $\sim 5 \times 10^{-3}$ Pa. The magnetron carbon target was high purity graphite disk 3 inch in diameter. Prior to deposition, quartz and c-sapphire substrates were cleaned by ultrasonically cleaning in methanol, acetone and deionised water to remove contaminants from the surface. Constant film deposition parameters were: flow of Ar - 25 sccm, N_2 - 8 sccm, working pressure 0.7 Pa, and magnetron input RF power 150 W at 13.56 MHz. Substrate holder temperatures was 900 °C. Tree series of samples was prepared with both types of substrates (quartz-Q, sapphire-S): Q1, S1 - without hydrogen, Q2, S2- hydrogen flow 1 sccm and Q3, S3 hydrogen flow 6 sccm. Elements concentration was determined by RBS (Rutherford backscattering spectrometry) and ERD (elastic recoil detection) methods simultaneously. Scanning Electron Microscopy (SEM) was used to investigate the surface morphology of carbon films. Raman spectroscopy using Raman microscope with 532 nm laser was used for chemical structural properties determination of carbon films. Electron beam evaporation was used for Ti contact frame preparation on structures. Fig. 1 shows main technological steps for transmission photocathode structure preparation. Bunch charge measurement of the prepared back side illuminated transmission photocathodes was made in JINR Dubna [1].

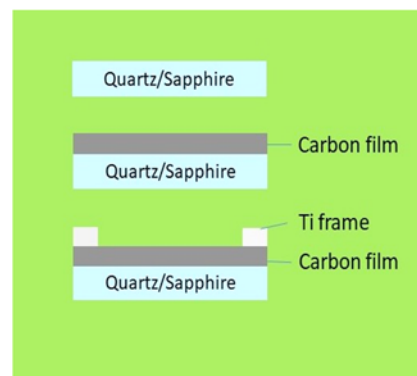


Fig. 1. Main technological steps for transmission photocathode structure preparation

3. Results and Discussions

Concentration of elements in the carbon films was calculated from RBS and ERD experimental spectra

using program SIMNRA. Elements concentration were practically the same in all samples and were: carbon~83 at.%, nitrogen~13 at.%, hydrogen~2 at.%, oxygen~2 at.%. Hydrogen in gas mixture not influences hydrogen concentration in the films. Concentrations of hydrogen are very small due to high substrate temperature i.e. hydrogen escapes from growing carbon films at 900 °C. We proposed that hydrogen and oxygen can be incorporated to the films after magnetron sputtering from the vacuum chamber wall during cooling of substrate holder and from air atmosphere. Fig. 2 shows SEM images of Q1, Q2, Q3 and S1, S2, S3 sample surfaces.

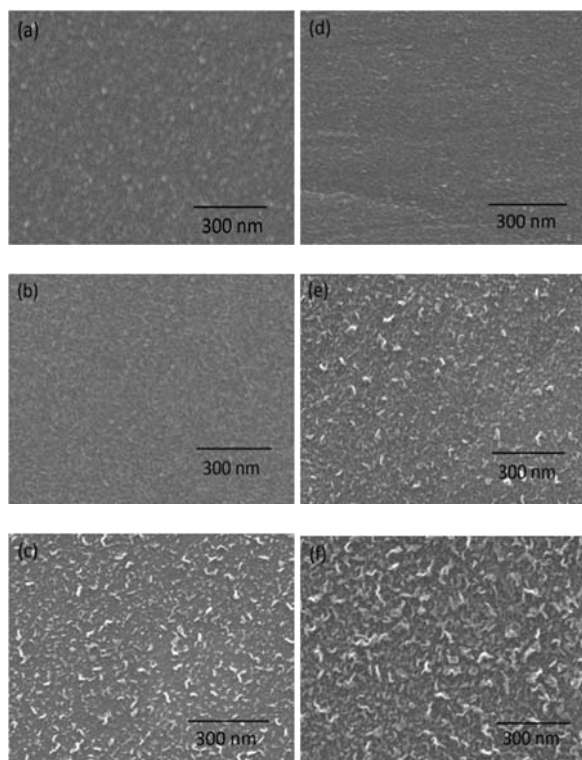


Fig. 2. SEM micrographs of samples surface: (a) - Q1, (b) - Q2, (c) - Q3, (d) - S1, (e) - S2 and (f) - S3.

Fully amorphous structure was observed for sample Q1. Amorphous structure was observed for samples Q2 and S1, but in these samples we can see start growth nano-scale thickness flakes. Nano-scale thickness flakes of random arrangement are shown on the surface of samples Q3, S2 and S3. Surface images of Q3 and S3 samples show no significance differences between their surface morphology. Only small difference of nano-scale thickness flakes dimension are shown. Added hydrogen to gas mixture had practically the same influence on carbon very thin films growth conditions on quartz or sapphire substrate. Hydrogen in gas mixture modifies parameters of film growth. Authors proposed that, at the start growth, the carbon atoms will grow a graphite and amorphous carbon film on substrate at nucleation site. When the carbon atoms are deposited on the

nucleation points, hydrogen will be etch more amorphous carbon. Then crystalline graphitic structures and the carbon nanosheet will be growing at the same time subsequently [13]. We proposed that crystalline graphitic structure start growth on surface of c-plane sapphire without adding hydrogen to gas mixture. Fig. 3 shows Raman spectra of all samples. Raman bands shapes for samples Q1, S1 is own for mixture of a-C, activated C and GNDC (graphite-like nanocrystalline diamond) [4]. Adding hydrogen to gas mixture Ar+N₂, Raman bands shape were change and can be assigned to the Raman spectra of mixture a-C, activated C, GNDC and small amount GSEC (graphene sheets embedded carbon) [3]. The D band and G band became distinct and narrow with increasing hydrogen flow. The 2D and D+G bands show practically plateau in the case of samples Q1 and S1. In the case of samples Q2, S2 and Q3, S3, bands 2D and D+G became clearer as a results of adding hydrogen to gas mixture.

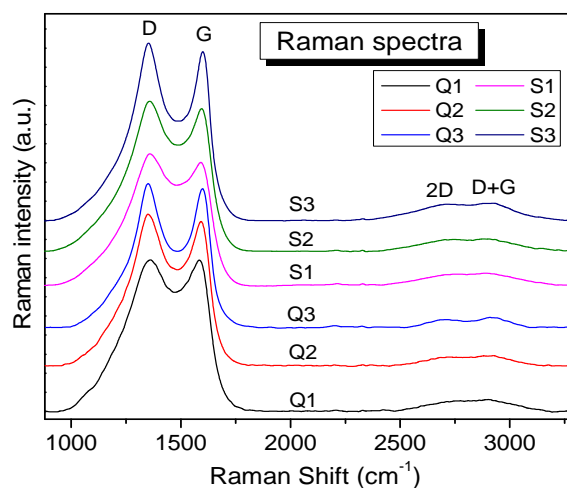


Fig. 3. Raman spectra for all samples in the range from 900 to 3300 cm⁻¹.

With more hydrogen flow, this effect continues. Raman spectra of carbon-based very thin films were Gaussian-fitted and identified. For the precision fitting, we used four peaks fitting for the range 1000-1800 cm⁻¹ and four peaks fitting for the range 2500-3200 cm⁻¹. Fig. 4 shows example of deconvoluted Raman spectra of sample S1. Fig. 5 shows example of deconvoluted Raman spectra of sample Q3. Peak intensities that occur at about 1200 cm⁻¹, 1350 cm⁻¹, 1580 cm⁻¹ and 1620 cm⁻¹ are called the ta-C, D, G and D' band, respectively. Peak intensities that occur at 2700 cm⁻¹ and 2940 cm⁻¹ are called 2D and D+G band. Peak ta-C can be assigned to tetrahedral amorphous carbon. The D band around 1350 cm⁻¹ is a breathing mode of A_{1g} symmetry involving phonons near the K zone boundary, which is activated due to defects and disorder of sp² carbon. The G band is a primary an in-plane vibrational mode. The D' band is attributed to another tensor of the A_{1g} mode [14].

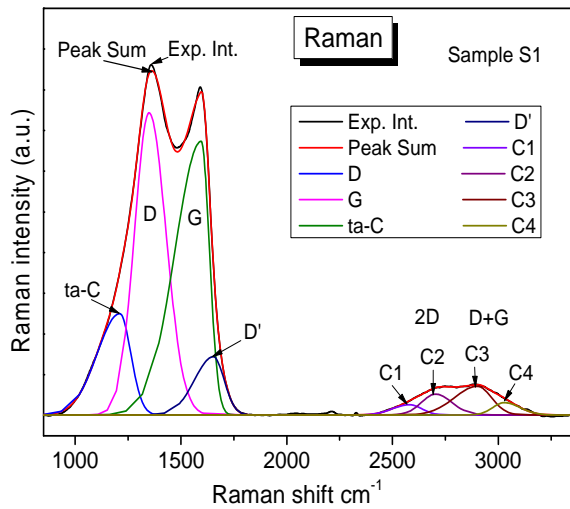


Fig. 4. Gaussians fitted Raman spectrum of carbon very thin film, sample S1.

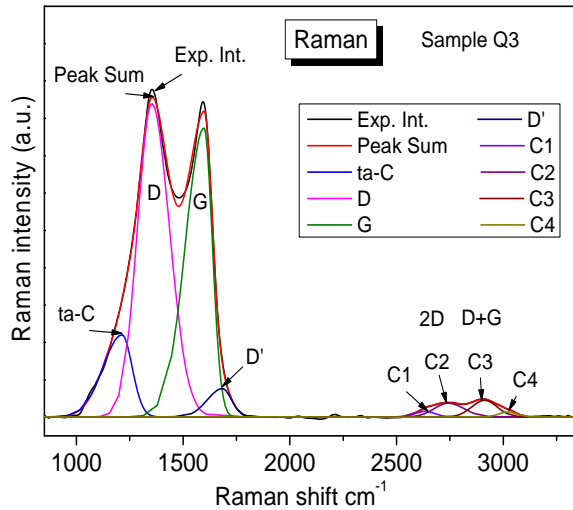


Fig. 5. Gaussians fitted Raman spectrum of carbon very thin film, sample Q3.

The 2D band, represented with peaks C1 and C2 is a second-order overtone of a different in-plane vibration [10]. We proposed that peak C2 at 2700 cm^{-1} is assigned to graphene-like carbon. The D+G band, represented with peaks C3 and C4 is a combination scattering peak and can be assigned to nanosized graphene sheets [15]. In Raman spectra is not shown feature at 2160 cm^{-1} which is assigned to sp^1 sites usually present in diamond-like carbon films. In Table 1 are present main calculated data from Raman spectra of all samples, as $I(D)/I(G)$ ratios and FWHM of D and G peaks. Adding hydrogen to gas mixture, results in decreasing of FWHM for D and G peaks for all samples, but are clear differences of $I(D)/I(G)$ ratios for Q samples. $I(D)/I(G)$ ratios are practically the same for S samples. The transmission photocathode quantum bunch charge measurements were performed at JINR Dubna. Transmission photocathode was back side illuminated with the 15 ns

UV laser pulses (quadrupled Nd:YAG laser, 266 nm) with laser spot size 5 mm.

Table 1. Calculated main data from Raman spectra.

Sample	$I(D)/I(G)$	FWHM (D)	FWHM (G)
Q1	1.44	186.3	174.8
Q2	0.92	166.2	156.7
Q3	1.31	154.5	123.9
S1	1.01	176.8	191.8
S2	0.99	175.6	190.1
S3	1.01	145.8	178.5

For the drawn of electrons from the carbon-based film coated quartz or sapphire photocathode a negative voltage was applied on the cathode. This voltage was kept at roughly 10-12 kV. The bunch charge was measured by using Faraday cup (FC). Samples were treated before bunch charge measurement by laser pulses during 10-40 min, for remove surface absorbed species from air atmosphere. We proposed that hydrocarbon and water contamination are removed with this type of degasing process from surface. Fig. 6 shows principal schema of photo-induced electron emission from transmission type photocathode. Parts of photons interact with carbon-based thin film and parts of photons transmit through photocathode structure without interaction. Laser radiation as the electromagnetic wave due to interaction with free electrons can penetrate into the material of the conductive film only to a depth of a skin layer. The estimated depth of the skin layer of graphite with conductivity $\sigma = (70-140) \times 10^3\text{ S/m}$ is about 50 nm for laser radiation at the wavelength $\lambda = 266\text{ nm}$. The mean free path of electrons in the material of the layer must be less than the value of the optical skin layer.

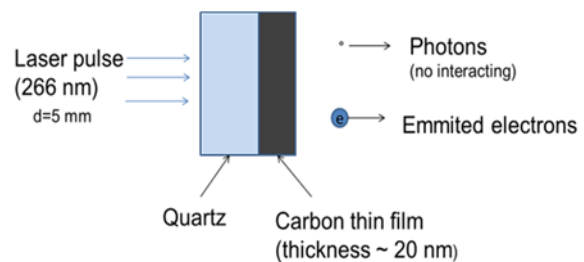


Fig. 6. Principal schema of photo-induced electron emission from transmission photocathode.

On the other hand mean free path of electrons depends not only on the skin effect but also on the scattering processes in the carbon-based materials. Optimal thickness for carbon-based very thin film was up to 25 nm, published in [16]. Small losses of laser photons energy are due to thickness of the substrate and its type. In our case the optical properties of quartz and sapphire for laser wavelength 266 nm are

practically the same. Electrical field for photo-induced electrons emission measurement was 1.5 kV/mm. The measured bunch charge and calculated quantum efficiency (QE) are present in Table 2. Results showed that adding small amount of hydrogen to the gas mixture, value of bunch charge rose up for Q substrate. More flow of hydrogen results in decreasing value of bunch charge. In the case of S substrate, adding hydrogen results in decreasing value of bunch charge. Maximum bunch charge and calculated QE(%) was 1.83 nC and 9.7×10^{-4} , respectively, and was for sample S1. In the case of Q samples, maximum bunch charge and calculated QE(%) was 1.14 nC and 6.1×10^{-4} , respectively, and was for sample Q2. One reason of worse results for quartz substrates can be explained by the higher stresses between quartz and carbon-based films result in more scattering centers for photoexcited electrons. This can be confirmed by results of I(D)/I(G) ratios assigned to more disordered carbon films for samples Q1 and Q3.

Table 2. The measured bunch charge and calculated QE.

Sample	Q1	Q2	Q3	S1	S2	S3
Bunch charge [pC]	930	1140	840	1830	1650	1310
QE(%) $\times 10^{-4}$	4.9	6.1	4.5	9.7	8.7	6.8

There existing several models for mechanism of photo-electron emission from carbon-based materials. Most of the published models related to reflective photocathode. In the case of back-side illuminated carbon-based transmission photocathode, the photo-emission characteristics depends not only on the doping and carbon film nanostructure but also on the thickness of film. Nanostructured carbon play important role as a results of containing several carbon phases with different work functions. Then the relationship between structural and electronic properties of the carbon-based films is yet uncertain.

4. Conclusions

For exploring the nanostructure effect on photo-induced electron emission properties of carbon-based very thin films, we prepared three types of carbon-based films on two types of substrates as quartz and sapphire. N-doped carbon-based very thin films were prepared by RF magnetron sputtering technology. Carbon films contain C, N and small amount of hydrogen and oxygen. SEM results showed no significant difference between sample surfaces prepared on both substrates for one series. Raman results showed interesting bands assigned to carbon based films as a-C, activated C, GNCD and very small amount of graphene-like carbon and graphene nanosheet embedded carbon. Maximum bunch charge

and $QE(\%) \times 10^{-4}$ were 1.83 nC and 9.7, respectively, and was for transmission photocathode S1. Reported results in this study call for detailed studies of carbon-based thin films structural properties to optimize the design and technology of carbon-based photo-induced electron emitters as a back-side illuminated transmission photocathode.

Acknowledgements

This research has been executed in the framework of the Topical Plan for JINR Research and International Cooperation (Project 02-0-1127-2019/2021) and supported by the Slovak Research and Development Agency under contract APVV-0443-12.

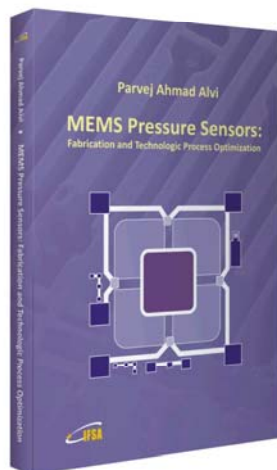
References

- [1]. N. I. Balalykin, V. F. Minashkin, M. A. Nozdrin, G. D. Shirkov, V. V. Zelenogorskii, E. I. Gacheva, A. K. Potemkin, J. Huran, Electron gun with a transmission photocathode for the Joint Institute for Nuclear Research photoinjector, *Physics-Uspekhi*, Vol. 60, 2017, pp. 1134-1141.
- [2]. L. Velardi, A. Valentini, G. Cicala, UV photocathodes based on nanodiamond particles: Effect of carbon hybridization on the efficiency, *Diamond & Related Materials*, Vol. 76, 2017, pp. 1-8.
- [3]. K. Sun, D. Diao, L. Yang, W. Zhang, X. Fan, Nanosized graphene sheets enhanced electron field emission behavior in pure carbon film, *Thin Solid Films*, Vol. 664, 2018, pp. 124-129.
- [4]. M. A. Nitti, M. Colasuonno, E. Nappi, A. Valentini, E. Fanizza, F. Bénédic, G. Cicala, E. Milani, G. Prestopino, Performance analysis of poly-, nano- and single-crystalline diamond-based photocathodes, *Nuclear Instrument and Methods in Physics Research A*, Vol. 595, Issue 1, 2008, pp. 131-135.
- [5]. V. I. Kleshch, D. A. Bandurin, P. Serbun, R. R. Ismagilov, D. Lützenkirchen-Hecht, G. Müller, A. N. Obraztsov, Field electron emission from CVD nanocarbon films containing scrolled graphene structures, *Phys. Status Solidi B*, Vol. 255, 2018, 1700270
- [6]. T. Sun, F. A. M. Koeck, P. B. Stepanov, R. J. Nemanich, Interface and interlayer barrier effects on photo-induced electron emission from low work function diamond films, *Diamond & Related Materials*, Vol. 44, 2014, pp. 123-128.
- [7]. A. Haque, J. Narayan, Electron field emission from Q-carbon, *Diamond & Related Materials*, Vol. 86, 2018, pp. 71-78.
- [8]. H. Li, Y. Xiong, B. Wang, B. Yang, N. Huang, Y. Liu, J. Wen, Microstructural modification of diamond-graphite nanohybrid films via adjusting deposition temperatures for enhanced electron field emission, *Diamond & Related Materials*, Vol. 87, 2018, pp. 228-232.
- [9]. J. Huran, N. I. Balalykin, A. A. Feshchenko, A. P. Kobzev, A. Kleinová, V. Sasinková, L. Hrubčín, Transmission photocathodes based on stainless steel mesh coated with deuterated diamond like carbon films, *Nuclear Instrument and Methods in Physics Research A*, Vol. 753, 2014, pp. 14-18.

- [10]. M. Inagaki, M. Toyoda, Y. Soneda, T. Morishita, Nitrogen-doped carbon materials, *Carbon*, Vol. 132, 2018, pp. 104-140.
- [11]. M. Mermouxa, S. Chang, H. A. Girard, J-Ch. Arnault, Raman spectroscopy study of detonation nanodiamond, *Diamond & Related Materials*, Vol. 87, 2018, pp. 248-260.
- [12]. M. S. Dresselhaus, A. Jorio, R. Saito, Characterizing graphene, graphite, and carbon nanotubes by Raman spectroscopy, *Annu. Rev. Condens. Matter Phys.*, Vol. 1, 2010, pp. 89-108.
- [13]. P.-T. Tseng, P.-H. Tsai, A. Lu, J.-L. Hou, H.-Y. Tsai, Field emission characteristic study on bristling few-layer graphite/diamond composite film, *Diamond & Related Materials*, Vol. 73, 2017, pp. 121-131.
- [14]. S. Takabayashi, H. Hayashi, M. Yang, R. Sugimoto, S. Ogawa, Y. Takakuwa, Chemical structure and electrical characteristics of diamondlike carbon films, *Diamond & Related Materials*, Vol. 81, 2018, pp. 16-26.
- [15]. B. B. Wanga, X. L. Qu, Y. A. Chen, K. Zheng, K. Ostrikov, Effects of plasma and gas flow conditions on the structures and photoluminescence of carbon nanomaterials, *Diamond & Related Materials*, Vol. 84, 2018, pp 178-189.
- [16]. N. I. Balalykin, J. Huran, M. A. Nozdrin, A. A. Feshchenko, A. P. Kobzev, V. Sasinková, P. Boháček, J. Arbet, Reactive magnetron sputtering of N-doped carbon thin films on quartz glass for transmission photocathode applications, *Journal of Physics: Conf. Series*, Vol. 992, 2018, 012031.



Published by International Frequency Sensor Association (IFSA) Publishing, S. L., 2019 (<http://www.sensorsportal.com>).



Hardcover: ISBN 978-84-616-2207-8
e-Book: ISBN 978-84-616-2438-6

So far, no book has described the step by step fabrication process sequence along with flow chart for fabrication of micro pressure sensors, and therefore, the book has been written taking into account various aspects of fabrication and designing of the pressure sensors as well as fabrication process optimization. A complete experimental detail before and after each step of fabrication of the sensor has also been discussed. This leads to the uniqueness of the book.

Features include:

A complete detail of designing and fabrication of MEMS based pressure sensor.

- Step by step fabrication and process optimization sequence along with flow chart, which is not discussed in other books.
- Description of novel technique (lateral front side etching technique) in terms of chip size reduction and fabrication cost reduction, and comparative study on both the techniques (i.e. Front Side Normal Etching Technology and Front Side Lateral Etching Technology) for the fabrication of thin membrane.
- Discussion on issues of sealing of conical tiny cavity; because the range of pressure applied (i.e. greater or less than atmospheric pressure) can be decided by methodology of sealing of tiny cavity.
- A complete theoretical detail regarding aspects of designing and fabrication, and experimental results before and after each step of fabrication.

MEMS Pressure Sensors: Fabrication and Process Optimization will greatly benefit undergraduate and postgraduate students of MEMS and NEMS courses. Process engineers and technologists in the microelectronics industry including MEMS-based sensors manufacturers.

Order: http://www.sensorsportal.com/HTML/BOOKSTORE/MEMS_Pressure_Sensors.htm